

## Palaeomagnetism of the Ordovician dolerites of the Crozon Peninsula (France)

H. Perroud and N. Bonhommet *Centre Armoricaïn d'Etude Structurale des Socles, LP 466 of CNRS, Laboratoire de Géophysique Interne, Université de Rennes 1, Campus de Beaulieu, 35042 Rennes-Cédex, France*

R. Van der Voo *Department of Geological Sciences, University of Michigan, Ann Arbor, Michigan 48109, USA*

Received 1982 April 20; in original form 1982 February 8

**Summary.** In order to obtain a Lower Palaeozoic pole for the Armorican Massif and to test the origin of the Ibero-Armorican arc, the Ordovician dolerites of the Crozon peninsula have been palaeomagnetically studied. The samples show a multicomponent magnetization which has been revealed by AF and thermal demagnetization and thoroughly investigated with rock magnetic experiments, polished section examinations and K/Ar dating. Four groups of directions have been recognized, often superimposed on each other in an individual sample. One component (D) has always the lowest blocking temperatures and coercivities and is considered to be of viscous origin, acquired recently *in situ* or in the laboratory during storage. Two components (A and B) are interpreted to be of secondary origin and to correspond to the observed K/Ar age distribution between 300 and 190 Myr. These ages represent the time interval between two regional thermo-tectonic events, associated with the Hercynian orogeny and the intrusion of dykes related to the early opening of the Central Atlantic Ocean and the Bay of Biscay. A fourth component (C) could be of Ordovician or younger Palaeozoic age; it is not clear whether the age of the magnetization is pre- or post-folding, but a pre-folding age would yield a direction of magnetization similar to Ordovician results from the Iberian peninsula. The latter interpretation suggests a fairly high palaeolatitude, which is in agreement with a glacio-marine postulated for sediments overlying the dolerite sills.

### Introduction

The Palaeozoic history of the Hercynian chain in Western Europe is still unclear and many geologists have proposed models of tectonic evolution for this orogeny, each quite different from the others. This chain exhibits features such as large widths, a great volume of syn-tectonic granites, an absence of ophiolitic series, presence of very marked shear zones, low-

or intermediate-pressure regional metamorphism and no clear tectonic characteristics of either a collisional or subduction type orogeny. Palaeomagnetic studies have begun in the Armorican Massif to study the pre-Hercynian history of Brittany in terms of movements of continental land masses, in the geodynamic context of the evolution of the major plates involved in the Hercynian orogeny. Thus, data have been obtained for the Eocambrian–Cambrian (Duff 1979, 1980; Hagstrum *et al.* 1980) and the Upper Devonian to Lower Carboniferous (Jones 1978; Jones, Van der Voo & Bonhommet 1979; Duff 1979; Van der Voo & Klootwijk 1972). Other studies are in progress at the Universities of Michigan and Rennes, but so far none have resulted in reliable palaeopoles for the Ordovician period. This is one of the reasons we sampled Ordovician volcanics in the Crozon peninsula. The second reason which led us to work there is its particular location in the Ibero-Armorican arc (Fig. 1a), a large-scale geological structure connecting the Hercynian massifs of Brittany and Spain across the Bay of Biscay, formed of large nested curved units. Stratigraphic studies, in particular, show excellent correlation between the Crozon and Buçaco synclines (Fig. 1a), where the Ordovician successions (Fig. 1b) can be well identified (Henry *et al.* 1974; Hamoumi, Le Ribault & Pelhote 1981). Some authors interpret this in palaeogeographic reconstructions as a proof that the two locations were in Ordovician time very near to one another, suggesting a quite different shape for the arc for pre-deformation times (Paris & Robardet 1977).

Therefore, a comparative palaeomagnetic study of the contemporaneous Ordovician volcanism in Crozon and Buçaco would enable us to test the role of the deformation in the present arc. We will present here the results obtained in the Crozon area, which forms part of a joint project of our two laboratories. A more detailed account of the work on the Palaeozoic origin of the Ibero-Armorican arc, including various locations, ages and rock-types, has been given in a thesis (Perroud 1980). Earlier, related conclusions for the origin of the arc have already been published (Perroud & Bonhommet 1981).

### Sampling and laboratory techniques

The Ordovician volcanism appears in the Crozon peninsula in two associated forms: large dolerite sills, interstratified in the sedimentary sequence (Fig. 1b and c) and a volcanic complex of the 'Pointe de Lostmarc'h' with an association of volcanic breccias, tuffs, pillow lavas and flows (Formation des Tuffs et calcaires de Rosan) palaeontologically dated as Upper Ordovician. This common Upper Ordovician age of the sills and the volcanics is based upon a cogenetic magmatism and the geometry of the intrusions. Because of difficult access to the outcrops, as well as fracturation and uncertainty about the structural position, the sampling has been concentrated on the dolerite sills; however, preliminary results obtained on hand samples of the pillow lavas have not shown other directions of magnetization than the ones reported here. Ninety-nine samples from 14 sites (Fig. 1c) have been drilled in the field, and oriented with magnetic and sun compasses, weather permitting, or by sighting on a far sea-mark (lighthouse, islands). Orientation errors are considered to be about  $\pm 2^\circ$  (Jones 1978).

The dolerite sills have been affected by Hercynian deformation, the first phase of which is the Bretonic phase (Visean). For the tilt correction, the stratification plane has been measured for the adjacent beds.

Natural remanent magnetization (NRM) measurements were made with a digital Schonstedt DSM-1 spinner. Alternating field (AF) demagnetizations were performed with a Schonstedt GSD-1 apparatus. The residual field in the shield is less than 10 nT; the generating signal is being monitored with an oscilloscope during the procedure. Thermal demagnetizations were done in a non-magnetic furnace (Schonstedt TSD-1) where the cooling takes

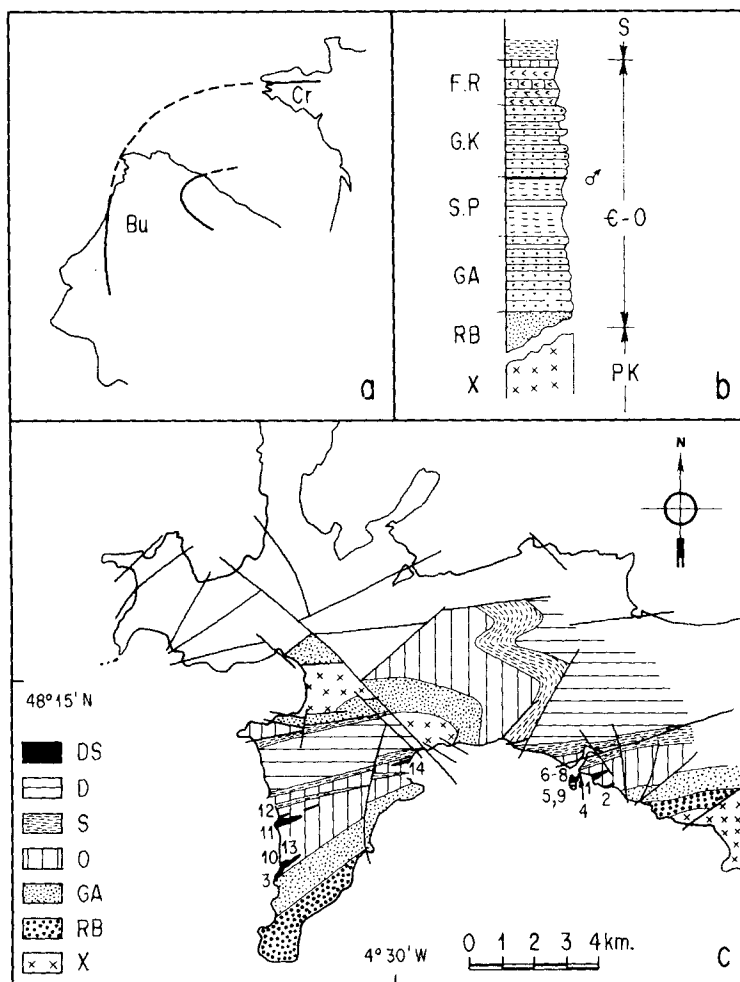


**Figure 1.** Geographical and stratigraphical framework of this study. (a) Geographical sketch of the Ibero-Armorican arc in a Permian configuration (Lefort 1980). Cr = Crozon, Bu = Buçaco. (b) Schematic stratigraphical sequence for late Precambrian (X = Brioverian) and early Palaeozoic times at Crozon; C = Cambrian, RB = red beds, GA = Grès Armoricaïn (early Ordovician), SP = Schistes de Postolonnec, GK = Grès de Kermeur, FR = Formation des Tufs et calcaires de Rosan, O = Ordovician, S = Silurian, D = Devonian, DS = dolerite sills. (c) Schematic geological map of the Crozon sampling area (after Barrière *et al.* 1975) with sampling sites.

place in a zero field chamber with the residual field also lower than 10 nT. Thermomagnetic experiments were also done, with Digico high- and low-temperature units.

## Results

### OPAQUE PETROLOGY AND K/AR DATES

Optical examination of thin sections (transmitted light) and polished sections (reflected light) reveal a titanomagnetite mineralogy. The opaque magnetic minerals are of large size (up to 1 mm), although often needle-shaped. Exsolution has resulted in relic ilmenite lamellae while the magnetite has generally been altered to non-opaque phases at intermediate

temperatures. A very advanced altered state of the original titanomagnetites is typical of these samples and makes the magnetic mineralogy complex.

There are no metamorphic minerals, and no structures related to the deformation can be found. But we must mention that there are no possible indicators of eventual reheating to temperatures lower than 300°C in such rocks.

K/Ar dating has been carried out on the freshest samples (measurements by J. Macé and Y. Leblanc at Rennes) and the results are given in Table 1. Individual ages are distributed between 190 and 300 Myr, irrespective of whether the samples came from the same site or not (see the four samples from site 1 in Table 1). Contamination effects from the edges of the sills cannot explain this dispersion, since sampling near the contact of the sills was avoided. On the other hand, the end members of this age distribution correspond to the ages of two major thermal events in the area (Hercynian general resetting at 300 Myr and late Triassic intrusion of dykes at 190 Myr). Thus, the dispersion could be due to a complex thermal history, which will certainly have had effects on the palaeomagnetic record (York 1978).

#### NRM RESULTS

The viscosity test (Thellier & Thellier 1959) has been applied to all specimens that have been sawed from the cores. Generally, specimens from the same core give identical results, but that was not the case for 20 per cent of the samples. This was the first suggestion of the complexity and sometimes the instability of the magnetization in these rocks. Intensities and the results of the laboratory (8 day) viscosity experiments are plotted in Fig. 2. Intensities show a good log-normal distribution, but with a large standard deviation about the very low mean value for such volcanic rocks ( $\sim 10^{-3} \text{ A m}^{-1}$ ). Viscosities are rather high since only 30 per cent of the samples give a viscosity coefficient lower than 10 per cent. This means that we can anticipate soft components in the demagnetization procedures, which would be parallel to the laboratory field in sample coordinates (samples are kept oriented in this field between experiments). NRM directions are generally somewhat scattered within a site, but the mean directions are quite coherent from site to site. We will return to the directions after a discussion of the demagnetizations since effects of the present-day field may not have been completely removed by the viscosity experiments (Prévot 1975). Two sites (6 and 12), giving

**Table 1.** Results of the K/Ar dating measurements (by J. Macé and Y. Leblanc) for the Crozon dolerites.

Site	Sample	Z K (Weight)	Weight (g)	$^{40}\text{Ar}^*$ ( $\text{cm}^3/\text{g}$ )	% Ar atmospheric	$^{40}\text{Ar}/^{36}\text{Ar}$			Age (Nyr)
						$^{40}\text{Ar}/^{36}\text{Ar}$	$^{40}\text{K}/^{36}\text{Ar}$	$^{40}\text{Ar}^*/^{40}\text{K}$	
1	78C04	0.366	0.79865	$4.71 \cdot 10^{-6}$	28	1055	39550	0.019	304
1	78C09	0.273	0.55067	$2.46 \cdot 10^{-6}$	32	915	45950	0.013	218
1	78C07	0.455	0.70556	$4.91 \cdot 10^{-6}$	8.7	3410	192920	0.016	260
1	78C01	0.655	0.52036	$8.45 \cdot 10^{-6}$	11.8	2500	114600	0.019	305
3	78C21	0.648	0.51753	$5.365 \cdot 10^{-6}$	9	3290	241840	0.0124	201
3	78C20	0.317	0.85362	$2.49 \cdot 10^{-6}$	24.4	1210	77760	0.0118	192
8	78C52b	0.443	0.69940	$5.41 \cdot 10^{-6}$	21.1	1400	60365	0.0183	290
11	78C81b	0.406	0.80950	$4.11 \cdot 10^{-6}$	28.4	1040	49310	0.0151	243
11	78C77b	0.445	0.80470	$4.27 \cdot 10^{-6}$	17.1	1725	99550	0.0144	232
9	78C59a	0.360	0.70620	$4.75 \cdot 10^{-6}$	14.6	2020	87540	0.0197	310
14	78C94b	0.360	0.81220	$4.33 \cdot 10^{-6}$	15.5	1910	89930	0.0180	285

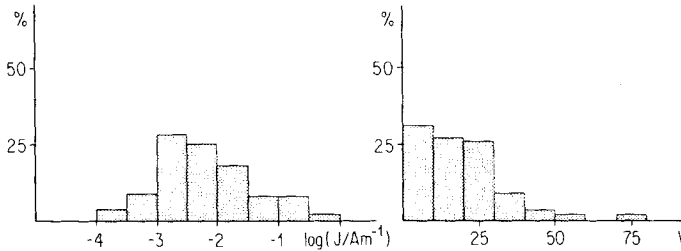


**Figure 2.** Frequency plots of the intensity of the NRM (left) and viscosity coefficients (see text) of the dolerites of Crozon (right).

only present-day field directions *in situ* and exhibiting clear evidence of oxidations (anomalous reddening, extensive alteration) have been rejected.

#### DEMAGNETIZATIONS

As a first step, pilot samples (about four for each site) were demagnetized progressively with increments lower than 10 mT in alternating fields and in steps of 50°C thermally. The observed behaviour led us to treat all other samples with alternating fields in four steps only (0, 20, 40 and 60 mT). Some AF and thermal demagnetization plots are shown in Figs 3 and 4. They illustrate the different behaviour exhibited by the samples. We can deduce several major features from these diagrams.

Some samples are not stable at any AF value, showing an erratic behaviour from step to step. No direction can be deduced (see for example 78C49 in Fig. 3). Nineteen specimens of the 76 treated have been rejected for this reason. Likewise, thermal demagnetization of a few specimens (four out of 25) does not allow us to distinguish any stable component, and the corresponding measurements have not been used.

A soft component is removed in AF demagnetization below 20 mT and in temperatures between 20° and 400°C. This component, in sample coordinates, is generally steep to very steep and downwards, corresponding to the present-day laboratory field. Moreover, the magnitude of this component is compatible with the 8 day viscosity coefficient: 38 per cent for sample 78C47, showing (Fig. 3) a large soft component, and 3 per cent for sample 78C87, for which this component does not appear. This component is, therefore, interpreted as a Viscous Remanent Magnetization (VRM), easily removed in AF demagnetization.

For high alternating field and temperature values, parasitic magnetizations (ARM?) or mineralogical changes (observed as a distinct brownish colour of the samples above 500°C) provoke anomalous behaviour (see samples 78C56 in Fig. 3 and 78C75 in Fig. 4). Hence, we could not determine any high-field or high-temperature magnetizations and we often had to terminate the demagnetization procedure at intermediate values of peak field or temperature.

Between 20 and 50 mT or 400° and 550°C, we could isolate one, sometimes two, directions of magnetization for the majority of samples, but generally demagnetization trajectories do not go to the origin. This means that the samples have at least two distinct magnetizations: the directions we were able to determine could correspond to discrete components or to vector sums. Since the spectra do not seem to be distinct, we cannot exclude the latter.

A few samples with high-intensity NRMs show a quite different behaviour, with a very fast decrease of the magnetization towards the origin (e.g. 78C87 in Fig. 3). Such behaviour is classically attributed to secondary Isothermal Remanent Magnetizations (IRM), for instance as a result of lightning.

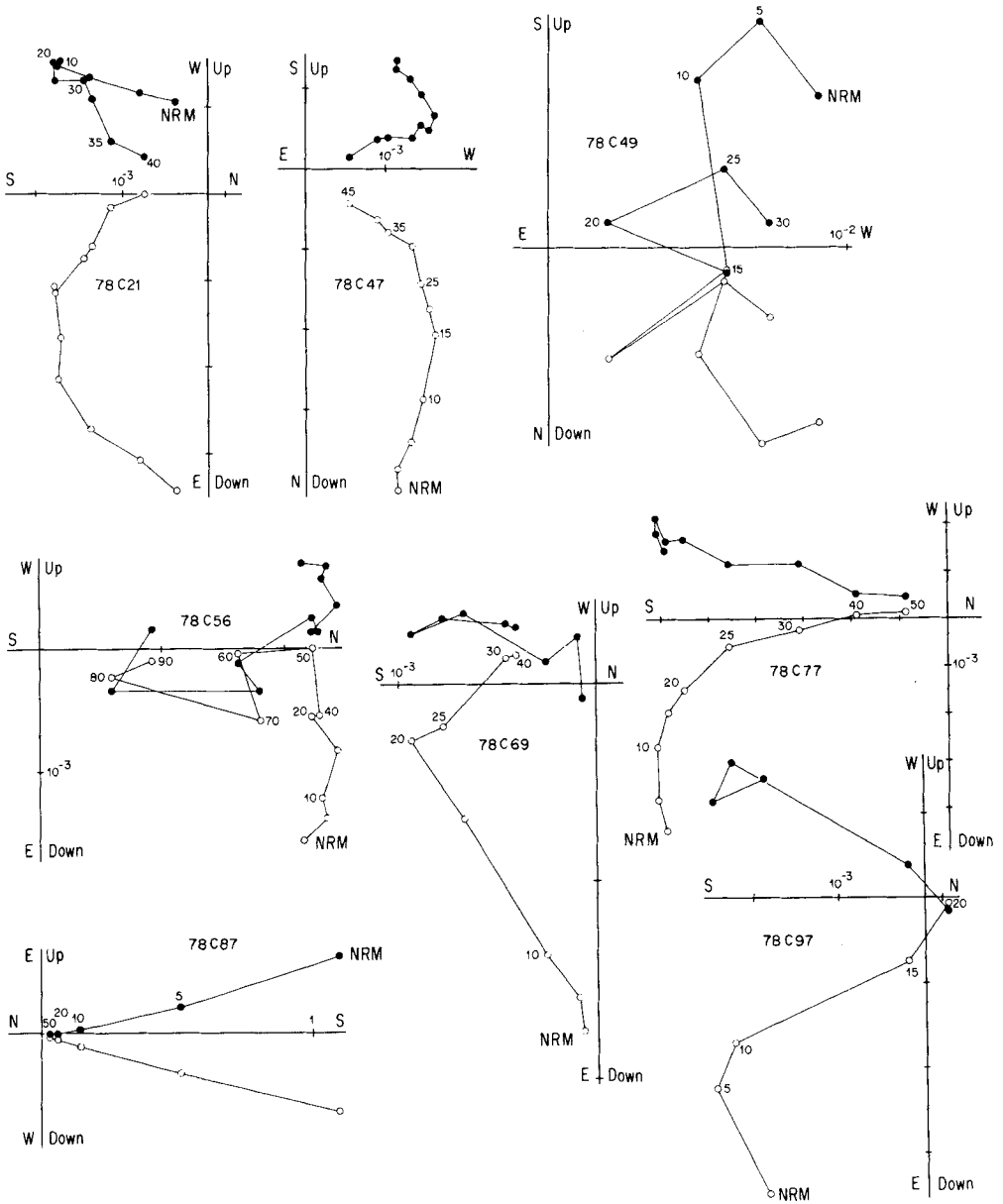


**Figure 3.** Demagnetization diagrams (Zijderveld 1967) for alternating field treatment. Intensity along the axes is in  $A\ m^{-1}$ . Solid circles represent projections on to the horizontal plane, and open circles those on the vertical plane. The plots are in *in situ* coordinates (without tilt correction).

### ROCK MAGNETISM

In contrast to the complex demagnetization diagrams, rock magnetic experiments give a simple picture of the magnetic mineralogy. IRM acquisition curves (Fig. 5a) are typical of magnetite, with saturation reached around 0.2 T, and coercivity spectra mainly compressed into fields lower than 0.1 T. Likewise, low-temperature treatment (cooling to liquid-air temperature of an IRM acquired at room temperature) very clearly reveals a magnetite

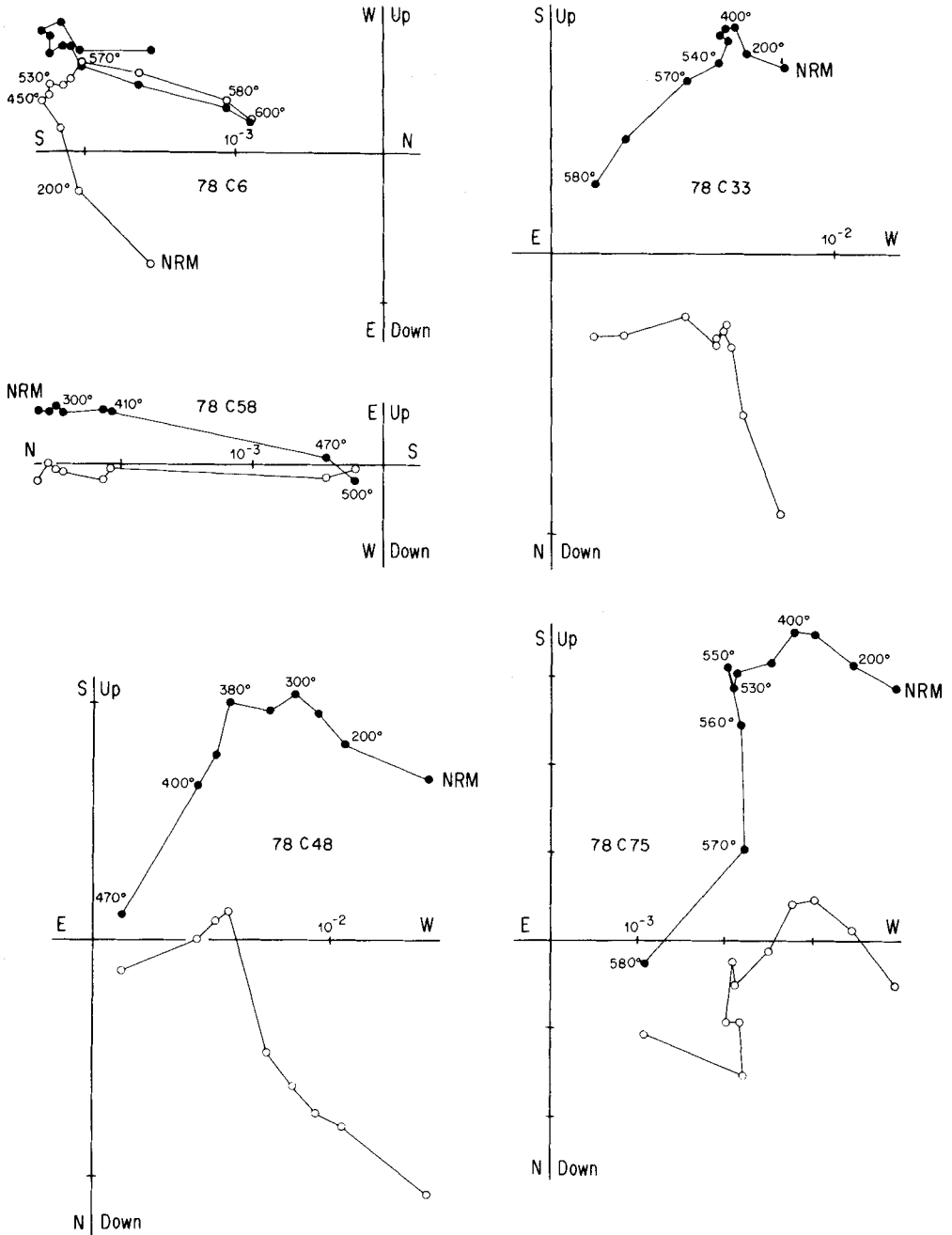


Figure 4. Demagnetization diagrams (as in Fig. 3) of thermally treated samples.

transition around  $-160^{\circ}\text{C}$  (Fig. 5b). There is no indication of possible other magnetic phases carrying a significant remanence. While opaque mineralogy studies have indicated the presence of some secondary magnetic minerals, the complex magnetization is likely to be carried by a single magnetic phase. The causes of this complexity are therefore to be searched in the history of the rocks rather than in a complex initial magnetic mineralogy.

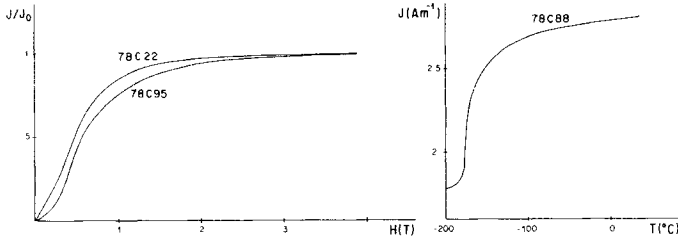


Figure 5. (a) Normalized intensity of Isothermal Remanent Magnetization versus applied field (in tesla). (b) Low temperature behaviour of Isothermal Remanent Magnetization, acquired at room temperature, showing a transition typical for magnetite. Intensity is in  $A\ m^{-1}$ .

Discussion of the results

Seventy samples (out of 99) give interpretable demagnetization diagrams; 80 directions have been identified, which are all different from possible recent viscous remanent directions. As we noted earlier, these data could correspond either to single components or to vectorial sums.

Two sites (9 and 14) exhibit an original coherent magnetization, well-grouped within and between the two sites, and do not show any other component (except for one sample of site 14). This direction is labelled as component C in Table 2 and has been plotted in Fig. 6(c). The mean direction computed from the 12 samples of these sites 9 and 14 and three samples from other sites, which are all north-westerly and shallow upwards, is  $D = 351^\circ$ ,  $I = -8^\circ$ ,  $k = 25$ ,  $\alpha_{95} = 7.7^\circ$  without tilt correction, and  $D = 356^\circ$ ,  $I = -64^\circ$ ,

Table 2. Summary of site-mean and group-mean palaeomagnetic directions.

Site	A-component				B-component				C-component				Strike and dip
	Decl./incl. before T.C.	Decl./incl. after T.C.	N	k	Decl./incl. before T.C.	Decl./incl. after T.C.	N	k	Decl./incl. before T.C.	Decl./incl. after T.C.	N	k	
1	202/-12	209/+36	4	25	217/+38	281/+55	2	130	352/+13	352/-42	1	-	263/55
2	198/-17	202/+33	2	7	229/+25	267/+41	2	75	343/- 5	334/-59	1	-	263/55
3	196/- 8	202/+24	4	14	211/+39	257/+42	4	18					239/49
4					223/+20	258/+44	6	31					263/55
5					224/+25	265/+45	2	18					263/55
7	220/-18	221/+21	2	21	244/+38	289/+34	2	118					263/55
8	223/-14	226/+22	4	8	241/+43	294/+38	1	-	5/+ 3	12/-50	1	-	263/55
9									351/- 9	349/-64	7	20	263/55
10	215/-15	211/+ 6	1	-	198/+34	244/+50	4	14					239/49
11	206/-20	202/+ 8	3	7	200/+12	220/+35	7	42					239/49
13					198/+12	219/+37	5	42					239/49
14					212/+25	254/+41	1	-	348/-14	12/-70	5	42	246/59
All samp.	207/-14		20	13	212/+25		36	15	351/- 8		15	25	
$\alpha_{95}$		210/+24	20	11		247/+44	36	13		356/-64	15	24	
	9.5	10.1			6.4	6.9			7.7	8.0			
All sites	209/-15		7	52	217/+29		11	21	352/- 3		5	37	
$\alpha_{95}$		211/+22	7	31		259/+45	11	18		355/-58	5	34	
	8.4	10.9			10.1	11.2			8.0	8.2			
Palaeo-pole	43N, 137E	25N, 142E	20		23N, 142E	55, 119E	36		37N, 187E	35, 178E	15		

Notes:

TC denotes tectonic correction,  $N$  is the number of statistical entries (directions of samples, or sites) used in the statistical analysis,  $k$  is the precision parameter and  $\alpha_{95}$  is the semi-angle of the cone of confidence of 95 per cent probability (McElhinny 1973). Strike and dip denote the bedding attitude measured at adjacent sedimentary strata at the site.



after tilt correction. The corresponding palaeopoles are located at  $37^{\circ}\text{N}$ ,  $187^{\circ}\text{E}$ , and  $3^{\circ}\text{S}$ ,  $178^{\circ}\text{E}$ , respectively. It cannot be decided, in the absence of a conclusive fold test, which of these palaeopoles is preferable. Consequently, the age of the magnetization could range from primary (Ordovician) to post-folding. In view of the European apparent polar wander path (Westphal 1976; French 1976), a post-Carboniferous age is very unlikely. It must be noted, however, that whenever the C magnetization coexists with another component (A, B or viscous) in an individual sample, it has the higher blocking temperatures or coercivities. Although no proof by itself, this argues for an interpretation in which the C magnetization is the oldest in our samples. If true, and assuming a pre-folding age of the magnetization, the palaeopole at  $3^{\circ}\text{S}$ ,  $178^{\circ}\text{E}$  implies a moderate to fairly high palaeolatitude. This in turn would agree very well with a glacio-marine origin postulated for sediments overlying the dolerites in Crozon (Hamoumi *et al.* 1981). Other evidence for tillites in Normandy, France (Dangeard & Doré 1971; Doré & LeGall 1972) and the Iberian peninsula (Robardet 1980), as well as moderate to high palaeolatitudes found in palaeomagnetic studies of rocks in Great Britain (Piper 1979) and in Spain and Portugal (Perroud & Bonhommet 1981), as well as in western Africa (e.g. Scotese *et al.* 1979), all point to a common history of these areas during the Ordovician.

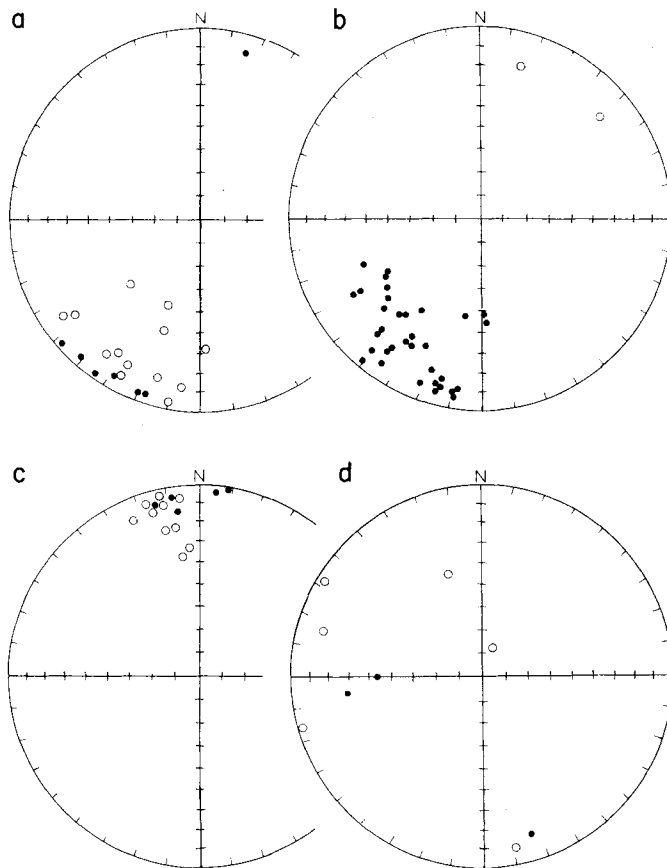


**Figure 6.** Equal-area projections of the directions obtained through vector analysis for samples from this study, plotted in *in situ* coordinates. (a) Group A directions. (b) Group B directions. (c) Group C directions. (d) Directions that are uninterpretable and do not belong to any other group. Open (solid) symbols represent projections on to the upper (lower) hemisphere.

All other directions have been plotted in Fig. 6(a, b, d). For clarity, the negative inclinations (mostly Group A in Fig. 6a) and positive inclination data (Group B) as well as nine random uninterpretable directions (Fig. 6d) have been plotted in separate equal-area projections, all in *in situ* coordinates. There are two ways in which to interpret the apparent distribution of the data of Groups A and B: either we have two distinct ages of ancient magnetizations or there is only one ancient component with the large scatter being an effect of recent viscous overprinting. In either case, some components do not fit the general repartition (Fig. 6d) and may be considered as parasitic or spurious magnetizations.

There are arguments in favour of either hypothesis for the distribution of directions of Groups A and B. The second hypothesis, in which this distribution is explained by a recent overprinting on an ancient south-westerly and up (?) direction, is supported by the fact that we often found evidence for viscous remanences aligned with the local present-day field (pdf). In some sites (7 and 8, for example), *in situ* directions can be considered to streak along a great circle between the Group A direction and the pdf. On the other hand, a strong argument for two ancient magnetizations exists in those demagnetization diagrams (Figs 3 and 4) where two well-defined directions can be isolated. In every case where both A and B magnetizations coexist, the B magnetization has higher blocking temperatures, whereas the coercivities are inconclusive: sometimes A is softer than B, other times B is the softer one (e.g. site 11).

Finally, the distribution of K/Ar dates between the ages of two regional thermo-tectonic events also favours the existence of two ancient components, because K/Ar systems are considered to have a dependence on temperature that is parallel to that of thermal remanent magnetizations (York 1978). Thus, we prefer the first assumption of two ancient magnetizations as a working hypothesis, but the possibility that the separation between the two components (A and B) is artificial will be kept in mind, as we analyse the directions in the next part of this section.

*A component*: this component (Fig. 6a) appears in seven sites, with two to four directions for each site and with moderate to low values of within-site  $k$  between 7 and 25 (Table 2). The Fisher statistics on the seven site-mean directions show a decrease of  $k$  from 52 to 31 upon tilt corrections (Table 2). Together with the K/Ar dates, and the similarity of these directions to the expected Permian directions for Europe, this leads us to postulate a post-folding Permian age for this component. The mean direction obtained from the 20 individual sample directions is  $D = 207^\circ$ ,  $I = -14^\circ$ ,  $N = 20$ ,  $k = 13$ ,  $\alpha_{95} = 9.5^\circ$ . The corresponding palaeopole is situated at  $43^\circ\text{S}$ ,  $317^\circ\text{E}$ , and falls on the apparent polar wander path for Europe (Fig. 7).

*B component*: this component (Fig. 6b) is the best represented one (36 directions from 11 sites). Within-site precision is high ( $k$  is generally  $> 20$ , see Table 2). Here as well, tilt corrections do not improve the statistical significance; this again is not surprising since the bedding attitudes for all the sites are fairly uniform. The similarity of the *in situ* mean direction to late Devonian and Carboniferous for Europe (Jones *et al.* 1979; Duff 1979) and the older K/Ar dates of 300 Myr lead us to suggest a possible Hercynian age for this component. Two possibilities remain: component B is a syntectonic magnetization or it is a pre-tectonic magnetization. The  $k$  values before and after tilt correction (15 and 13) do not allow us to distinguish between these two alternatives. The mean directions yield palaeopoles at  $23^\circ\text{N}$ ,  $142^\circ\text{E}$  (without tilt correction) and  $5^\circ\text{S}$ ,  $119^\circ\text{E}$  (after tilt correction). These poles labelled B and B', respectively, have been plotted in Fig. 7 with the apparent polar wander path for Europe. Pole B is very close to the early Carboniferous poles of Europe, which is quite consistent with a syn- to late-tectonic acquisition of the magnetization. On the other hand, pole B' does not fit the path for late Palaeozoic time, nor does it fit with early Palaeozoic poles determined so far for the Armorican Massif (Duff 1980; Hagstrum

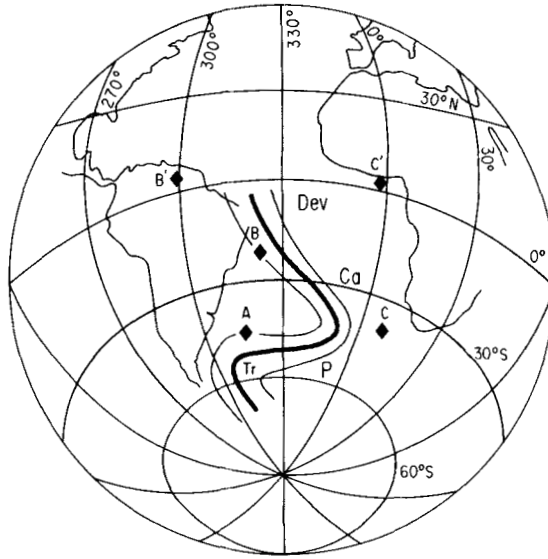


**Figure 7.** The apparent polar wander path for the late Palaeozoic and early Mesozoic for Europe (after Westphal 1976; French 1976; Duff 1980), with the palaeopoles obtained in this study. Dev = Devonian, Ca = Carboniferous, P = Permian and Tr = Triassic.

*et al.* 1980). Ordovician palaeopoles from other parts of the Ibero-Armorican arc (Perroud & Bonhommet 1981) are also quite different from pole B'. Finally, the K/Ar dates are limited towards the oldest ages at 300 Myr, which is the age of Hercynian thermo-tectonic events and of the syntectonic intrusion of granites in the Armorican Massif. For all these reasons, the syntectonic model is preferred, implying that the B component would have been acquired at a late stage of the deformation. Apparently, an orogenic setting is very favourable to a resetting of magnetizations. Hence, the assumption that two older magnetizations coexist in our rocks agrees with an association of the components with the oldest and youngest of the K/Ar ages, which in turn represent the two major regional thermal events.

## Conclusions

Our palaeomagnetic study of the Ordovician dolerites of the Crozon peninsula shows a complex magnetization. Three distinct ancient components (A, B and C) have been found, which lead to three palaeopoles compatible with the apparent polar wander path for Europe between the Ordovician and the Triassic. Two components (A and B) are interpreted in relation to K/Ar dates between 300 and 190 Myr. The third (C) component could be of Ordovician age with  $D = 356^\circ$ ,  $I = -64^\circ$ , or alternatively, of a post-folding, late Palaeozoic age with  $D = 351^\circ$ ,  $I = -8^\circ$ . In view of the apparent polar wander path of Europe, an age of this magnetization younger than Carboniferous seems to be extremely unlikely. We note that, if this C-magnetization is of Ordovician age, it agrees very well with Ordovician palaeopoles for Great Britain (Piper 1979) and is close to directions reported by Perroud & Bonhommet (1981) for northern Spain and Portugal. Moreover, its steep upward direction suggests a position fairly close to the palaeopole. In terms of early Palaeozoic continental reconstructions, this interpretation of our C-magnetization implies a position of the Armorican Massif fairly close to that of southern England and Wales, as well as to

Gondwana, as noted by Perroud & Bonhommet (1981), as well as Hagstrum *et al.* (1980) for earlier, late Precambrian to Cambrian, time.

### Acknowledgments

J. J. Chauvel and H. P. Johnson are thanked for their help in the optical examination of the samples, and so are J. Macé and Y. Leblanc for the K/Ar dating measurements. H. P. Johnson is also thanked for a critical reading of the manuscript and for helpful comments. This work was supported by a grant of INAG through the National Research Program 'A.T.P.-Géodynamique'.

### References

- Barrière, C. *et al.*, 1975. Carte géologique de la France au 1/50,000 et notice, *Feuille Douarnenez*, no. 309, Bureau de Recherche Géologique et Minière, Paris.
- Dangeard, L. & Doré, F., 1971. Faciès glaciaires de l'Ordovicien supérieur en Normandie, *Mém. Bur. Rech. Géol. Min.*, **73**, 550–565.
- Doré, F. & LeGall, J., 1972. Sédimentologie de la "Tillite de Feugerolles" (Ordovicien supérieur de Normandie), *Bull. Soc. géol. Fr.* (7), t. **XIV**, 199–211.
- Duff, B. A., 1979. The palaeomagnetism of Cambro-Ordovician red beds, the Erquy spilite series, and the Trégastel-Ploumanac'h granite complex, Armorican Massif (France and the Channel Islands), *Geophys. J. R. astr. Soc.*, **59**, 345–365.
- Duff, B. A., 1980. The palaeomagnetism of Jersey volcanics and dykes and the Lower Palaeozoic apparent polar wander path for Europe, *Geophys. J. R. astr. Soc.*, **61**, 355–375.
- French, R. B., 1976. Lower Palaeozoic paleomagnetism of the North American craton, *PhD thesis*, University of Michigan, Ann Arbor.
- Hagstrum, J. T., Van der Voo, R., Auvray, B. & Bonhommet, N., 1980. Eocambrian–Cambrian palaeomagnetism of the Armorican Massif, France, *Geophys. J. R. astr. Soc.*, **61**, 489–517.
- Hamoumi, N., Le Ribault, L. & Pelhate, A., 1981. Les Schistes de Cosquer (Ordovicien supérieur, Massif Armoricain occidental): une formation glacio-marine à la périphérie d'un inlandsis ordovicien, *Bull. Soc. géol. Fr.* (7), t. **XXIII**, 279–286.
- Henry, J. L., Nion, J., Paris, F. & Thadeu, D., 1974. Chitinozoaires, Ostracodes, et Trilobites de l'Ordovicien du Portugal (Serra de Buçaco) et du Massif Armoricain: essai de comparaison et signification paléogéographique, *Comunicações Servs geol. Port.*, **57**, 305–345.
- Jones, M., 1978. Paleozoic paleomagnetism of the Armorican Massif, France, *MSc thesis*, University of Michigan, Ann Arbor.
- Jones, M. Van der Voo R. & Bonhommet, N., 1979. Late Devonian and early Carboniferous palaeomagnetic poles from the Armorican Massif, France, *Geophys. J. R. astr. Soc.*, **58**, 287–308.
- Lefort, J. P., 1980. Un fit structural de l'Atlantique Bord: arguments géologiques pour corréler les marqueurs géophysique reconnus sur les deux marges, *Mar. Géol.*, **37**, 355–369.
- McElhinny, M. W., 1973. *Paleomagnetism and Plate Tectonics*, Cambridge University Press, 358 pp.
- Paris, F., 1980. Les chitinozoaires dans le Paléozoïque de Sud Ouest de l'Europe, *Mém. Soc. géol. minér. Bretagne*, **26**, 410 pp.
- Paris, F. & Robardet, M., 1977. Paléogéographie et relation ibéro-armoricaine au Paléozoïque anté-Carbonifère, *Bull. Soc. géol. Fr.* (7), t. **XIX**, 1121–1126.
- Perroud, H., 1980. Contribution à l'étude paléomagnétique de l'arc IbéroArmoricain, *thèse 3e cycle*, University de Rennes, and *Bull. Soc. géol. minér. Bretagne*, **C, 14**, 1–114 (1982).
- Perroud, H. & Bonhommet, N., 1981. Palaeomagnetism of the Ibero-Armorican arc and the Hercynian orogeny in western Europe, *Nature*, **292**, 445–448.
- Piper, J. 1979. Aspects of Caledonian palaeomagnetism and their tectonic implications, *Earth planet. Sci. Lett.*, **44**, 176–192.
- Prévot, M., 1975. Magnétisme et minéralogie magnétique de roches néogènes et quaternaires, contribution au paléomagnétisme et à la géologie du Velay, *thèse de Doctorat*, University of Paris.
- Robardet, M., 1980. Late Ordovician tillites in the Iberian peninsula, in *Earth's pre-Pleistocene Glacial Records*, pp. 131–134, eds Hambrey, M. G. & Harland, W. B., Cambridge University Press.
- Scotese, C. R., Bambach, R. K., Barton, C., Van der Voo, R. & Ziegler, A. M., 1979. Paleozoic base maps, *J. Geol.*, **87**, 217–277.

- Thellier, E. & Thellier, O., 1959. Sur l'intensité du champ magnétique terrestre dans le passé historique et géologique, *Ann. Géophys.*, **15**, 285–376.
- Van der Voo, R. & Klootwijk, C. T., 1972. Paleomagnetic reconnaissance study of the Flamanville granite, with special reference to the anisotropy of its susceptibility, *Geol. Mijnb.*, **51**, 609–617.
- Westphal, M., 1976. Contribution du paléomagnétisme a l'étude des déplacements continentaux autour de la Méditerranée occidentale, *thèse de Doctorat*, University of Strasbourg.
- York, D., 1978. A formula describing both magnetic and isotopic blocking temperatures, *Earth planet. Sci. Lett.*, **39**, 89–93.
- Zijderveld, J. D. A., 1967. AC demagnetization of rocks: analysis of results, in *Methods in Paleomagnetism*, pp. 254–287, eds Collinson, D. W., Creer, K. M. & Runcorn, S. K., Elsevier, New York.